Nigerian Journal of Technology (NIJOTECH)
Vol. 44, No. 1, March, 2025, pp.39 - 47
www.nijotech.com

Print ISSN: 0331-8443
Electronic ISSN: 2467-8821
https://doi.org/10.4314/njt.v44i1.5

KINETIC AND THERMODYNAMIC STUDIES OF THE DEVOLATILIZATION OF PUMPKIN PODS (*Telfairia occidentalis Hook F.*) WASTES

AUTHORS:
N. R. Agbale[1], M. U. Ajieh[2,*] G. O. Atonuje[3], K. O. Adiotomre[4], S. N. Eze[5], D. Atugba[6] and I. F. Okafor[7]

AFFILIATIONS:
[1,2,3,4,5,6]Department of Chemical Engineering, Delta State University, Nigeria
[7]National Centre for Energy Research and Development, University of Nigeria, Nsukka, Enugu State, Nigeria

***CORRESPONDING AUTHOR:**
Email: mike.ajieh@gmail.com

ARTICLE HISTORY:
Received: 15 June, 2024.
Revised: 05 November, 2024.
Accepted: 18 November, 2024.
Published: 14 April, 2025.

KEYWORDS:
Pumpkin pods, bio-fuels, energy generation, pyrolysis, kinetic models, thermodynamic parameters.

ARTICLE INCLUDES:
Peer review

DATA AVAILABILITY:
On request from author(s)

EDITORS:
Chidozie Charles Nnaji

FUNDING:
None

Abstract

Waste accruing from Pumpkin pod (Telfairia occidentalis Hook F.) was exposed to pyrolysis at varying temperatures namely; 350^{o}C, 400^{o}C, 500^{o}C and 600^{o}C and the heating rates were monitored at 0.17, 0.33 and 0.5 ^{o}C/sec. The biochar were then characterized in terms of yield, proximate composition and the process kinetics evaluated using Flynn-Wall-Ozawa (FWO), Kissinger-Akahira-Sunose (KAS) and Starink models. The models also showed the behaviour of the biochar with respect to to change in temperature. Proximate analysis of the biochar shows that it contains 11.77% moisture, 2.64%ash 12.50% fixed carbon and 73.10% volatile matter with a heating value of 17.91 MJ/kg. Furthermore, at 10^{o}C/min, 20^{o}C/min and 30℃/min, the biochar yield (wt%) decreased from 63.1 to 42.13, 59.87 to 38.33 and 51.91 to 32.12 respectively as pyrolysis temperature increased from 350^{o}C to 600^{o}C. FWO, KAS and Starink models, show high R^2 squared values greater than 0.9400, which indicate a good fit of the models. The mean activation energy (E_A) obtained for FWO, KAS and Starink models were 157.68kJ/mol, 157.23kJ/mol and 157.38kJ/mol. The thermodynamics results for FWO, KAS and Starink models show an average enthalpy of 152.30kJ/mol, 157.44kJ/mol and 155.14KJ/mol, average free energy of 112.89kJ/mol, 122.77kJ/mol and 116.73kJ/mol and low average entropy of 0.077kJ/mol, 0.075kJ/mol and 0.073kJ/mol. The optimization of the thermal conversion of pumpkin pod for energy and sequestration purposes is provided by the theoretical analysis of this study.

1.0 INTRODUCTION

Energy is one of the most critical factors that contribute to the advancement of a nation's development. The availability and adequate provision of energy is an essential requirement in the quest for better living conditions. The high requirement for energy is a result of the growing global population in addition to emerging industries and advancements across subfields [1]. In order to meet the current high energy demands, other energy sources are being researched as alternatives to fossil sources which are known to be depleting in reserves and also cause challenges of greenhouse emissions. In developing countries, there has been an increase in the studies of converting biowaste to fuels, so as to meet the demands of an increasing population and cleaner environment [2].

Biofuels which could be solids, liquids or gases are generally cleaner burning than petroleum fuels made from crude oil. They may be considered carbon-

HOW TO CITE:
Agbale, N. R., Ajieh, M. U., Atonuje, G. O., Adiotomre, K. O., Eze, S. N., Atugba, D., and Okafor, I. F. "Kinetic and Thermodynamic Studies of the Devolatilization of Pumpkin Pods (*Telfairia occidentalis Hook F.*) Wastes ", *Nigerian Journal of Technology*, 2025; 44(1), pp. 39 – 47; *https://doi.org/10.4314/njt.v44i1.5*

neutral because the plants that are used to make biofuels (such as corn and sugarcane for ethanol and soy beans and oil palm trees for biodiesel) absorb CO_2 as they grow and may offset the CO_2 emissions when biofuels are produced and burned [3]. The biomass from agricultural waste is a promising source of substitutes of conventional fuels because of their high energy potential and high carbon content [4], [5]. Among the various types of agricultural waste, those from bean crops (represented by straw and pods) is highlighted because it is produced in large amounts as the result of grain processing [6]. Because these residues require a significant amount of time to be naturally degraded and absorbed in the soil, several studies investigated the reuse of these types of biomasses in the generation of products with aggregated value [7].

Pyrolysis occurs between 300ºC and 700ºC and converts biomass into biofuels and biochar. This process is significant for managing hazardous waste, soil remediation and as well as carbon sequestration [8]. The design of pyrolytic reactions as well as the mechanism of the reactions are evaluated by the kinetic and thermodynamic analysis of the process for optimal output. Therefore, this study looks at the production of liquid and solid biofuels by subjecting pretreated pumpkin pods to the pyrolytic process. The resultant properties of the process were further investigated using kinetic models.

2.0 MATERIALS AND METHOD

2.1 Pre-treatment of Pumpkin Pod (PP)

Fresh empty PP which were sourced from Eku local market in Ethiope East Local Government Area, Delta State, Nigeria and washed thoroughly to eliminate the dirt particles and dusts. The PP were sun-dried for one week, care was taken to leave them in a well-aerated environment. This to avoid the growth of moulds, which may denature the PP. They were thereafter, reduced to sizes of about 4cm by 4cm using knives and cutters.

2.2 Production of Biochar by the Pyrolytic Process

The pyrolytic process was conducted in line with Mohan et al. [8], 10g each of the dried PP was transferred to a stainless-steel tray and transferred to a muffle furnace (Model: SNOL 1,6,5.1/11 Ceramic, India) set at a temperature of 350°C. Nitrogen was continuously passed through the furnace to purge the furnace of oxygen at 0.2 ml/minute. The process was ramped at 30 ºC/minute. This experiment was repeated at 400, 500 and 600 ºC. The resultant products of the reaction were present in all three phases. Oil from each of the processes was extracted from the aqueous fraction and the mass of each fraction was taken before and after heat treatment at each temperature to ascertain the total mass of the fuel products [9].

2.3 Analysis of Fuel Constituents

The solid and bio-oil yields at different temperatures were obtained using Equation 1 and 2.

$$Char\ yield\ (\%) = \frac{mass\ of\ char}{mass\ of\ pods} \times 100\% \quad (1)$$

$$Oil\ yield\ (\%) = \frac{mass\ of\ oil}{mass\ of\ pods} \times 100\% \quad (2)$$

Proximate analysis was conducted on the PP and pumpkin pod biochar (PPB) pyrolyzed at 350, 400, 500 and 600 ºC) using LECO TGA 701 (USA) based on the ASTM D5142 method [26].

2.4 Thermal Properties

The thermal behaviour of the biochar pyrolysed at 500ºC was examined following the standard procedure outlined in ASTM E113 [27]. The analysis was performed using a Shimadzu DTA-50 analyzer at 0.17, 0.33 and 0.5ºC/sec from 0 to 900ºC in inert conditions using N_2 gas at a flow rate of 20 ml/min. First, 20mg of weighted samples were heated from 30°C to 100°C until complete dehydration was established. This was followed by the decomposition reaction at 600°C for 7 minutes to monitor the quantity of volatile matter. The atmosphere was oxidized at the final stage to determine the percentage composition of the fixed carbon. The oxidation reaction was allowed to progress until the solid reached a constant mass percent [10].

2.5 Kinetics of Biochar Synthesized at 500ºC

The thermal decomposition kinetics of pumpkin pod biochar pyrolyzed at 500 (PPB-500) can be expressed as the differential equation of the mass transfer functions and mass fraction derivatives [28]. It follows the reaction (Equations 3-11):

PPB-500 = fixed carbon + (L + G) volatile (3)

For a reaction which occurs at an unsteady temperature in a multi-phase system, the conversion of the biochar (PPB-500):

$$\frac{dx}{dt} = k_p f(x) \quad (4)$$

Where, x = conversion, t = time, k_p = kinetic rate constant, f(x) = reaction model conversion factor.

$$f(x) = (1 - x)^n \text{ and;} \quad (5)$$

$$x = \frac{m_0 - m_t}{m_0 - m_f}, \quad (6)$$

n = order of reaction, m_o = initial mass, m_t = mass at specific time t, m_f = mass of PPB-500. The Arrhenius theory is given in terms of k_p as; $k_p = Ae^{\frac{-\varepsilon_A}{RT}}$; A = Arrhenius pre-exponential factor (1/s), T = reaction temperature (K), ε_A = activation energy in kJ/mol, and R is the universal gas constant represented as 8.314 J/mol/K. Thus, substituting Arrhenius equation gives;

$$\frac{dx}{dt} = Ae^{\frac{-\varepsilon_A}{RT}} f(x) \quad (7)$$

For an increase in temperature at a given rate, β = dT/dt or Tt = T_0 + βt.

Substituting dt = $\frac{dT}{\beta}$ into Equation 7, the time derivative is changed to the temperature derivative (Equation 6) [11], [12],

$$\frac{dx}{dT} = A/\beta e^{\frac{-\varepsilon_A}{RT}} f(x) \quad (8)$$

Flynn–Wall–Ozawa (FWO) [29], Kissinger–Akahira–Sunose (KAS) [30] and the Starink [31] models were used in the evaluation of the kinetic properties. The FWO method expressed in Equation (9) shows that ln(β) and 1/T are directly related at various conditions of β at different temperatures. The slopes of the plots of equation (9) were used to compute the activation energies [12].

$$l \cap \beta = \frac{ln\, A\epsilon_A}{f(x)R} - 5 \cdot 331 - 1.052\frac{\epsilon_A}{RT} \quad (9)$$

The KAS model expressed in Equation (10) gives a linear relationship between (lnβ/T^2) and 2/T in which E_A is obtained from the gradient of the plot as shown in Equation 8;

$$L_n\left(\frac{\beta}{T^2}\right) = ln\left(\frac{A\epsilon_A}{g(x)R}\right)\frac{\epsilon_A}{RT} \quad (10)$$

The Starink model is similar to the KAS and the FWO. Equation (11) is applied in the estimation of ϵ_A

$$ln\left(\frac{\beta}{T^{1\cdot92}}\right) = C - 1.0008\left(\frac{\varepsilon_A}{RT_A}\right) \quad (11)$$

The plots of $ln\left(\frac{\beta}{T^{1\cdot92}}\right)$ against $\frac{1}{T}$ gives a slope of $1.0008\left(\frac{\varepsilon_A}{RT_A}\right)$

2.6 Thermodynamic Properties of PPB-500

The average activation energy from FWO and KAS models were used to compute the thermodynamics properties e.g., enthalpy, ΔH, pre-exponential factor, A, entropy ΔS and Gibbs free energy ΔG as shown in Equations 10 - 13.

$$A = \frac{\beta e^{-\epsilon_A/Tm}}{RT_m 2} \quad (10)$$

$$\Delta H = \epsilon_A - RT \quad (11)$$

$$\Delta G = \epsilon_A - RTm\, ln\left(\frac{k_B RT}{hA}\right) \quad (12)$$

$$\Delta s = \frac{\Delta H - \Delta G}{T_m} \quad (13)$$

Where, T_m is the maximum decomposition temperature at DTG peak, K_B is Boltzmann constant (1.381 x10^{-23} J/K), and h is the Planck's constant (6.626 x 10^{-34} J/s).

3.0 RESULTS AND DISCUSSION

3.1 Biomass Characterization

The composition analyses of fresh and dried pumpkin pod (*Telfaira occidentalis* Hook F.) are given in Table 1. Essentially, the bulk density and/or mechanical durability during storage and transportation have direct relationship with the amount of moisture present in a material [13]. Research has shown that for significant thermal efficiency, a moisture content of 11 – 13% for storage over four months is preferred [13]. In other words, moisture is one of the main factors influencing biomass performance as fuel, this is due to energy losses during drying, thus leading to a considerable decline in calorific value [14]. To say the least, higher moisture implies a decrease in the thermal energy of the precursor combustion [15]. The moisture of the fresh PP was found to be 90.8% which indicates a high moisture. The dried PP, however, contained 11.77% which indicates that the dried pod can be stored and transported over some time. Ash is the solid residue left after the volatile matter is completely burned. Table 1 shows that the ash content of the fresh and dried fluted pumpkin pods is 0.50 and 2.64% respectively. This increase may be attributed to a decrease in the moisture content of the pod as a reduction in moisture aids carbonization. Moreover, the level of volatile matter is predicated on the amount of smoke or gas produced during combustion and thus, facilitates ignition as a result of flammable organic compounds [5]. The volatile matter of the dried pumpkin pod is found to be 73.10% while the fixed carbon, known as the solid carbonaceous residue from drying and devolatilization is used to estimate the coke (coking) potential [16] of carbonaceous materials and in this case, the fixed carbon obtained is 12.50%.

Table 1: Composition of fresh and dried PP

Nutrient Fraction	Undried (wt %)	Proximate content	Dried (wt %)
Moisture content	90.80	Moisture content	11.77
Protein	1.38	Ash	2.64
Fibre	0.84	Fixed carbon	12.50
Ash	0.50	Volatile matter	73.10
Ether extract	0.60		
Nitrogen-free extract (NFE)	5.88		

3.2 The Dependency of Yield on Temperature and Heating Rates

The biochar and bio-oil yields is as shown in Figure 1. Heating rate a vital parameter used in the description of the types of pyrolytic process (slow, fast, flash, etc.). Bio-chars derived from varying heating rates display diverse distributions of the functional groups and have different porosities and surface areas which are of vital importance for the effectiveness of bio-char for soil amendment [17], [18]. More so, an increase in the heating rate from 10 to 30℃/min had a considerable effect on bio-char yield from 350℃ to 600℃. In other words, 283Kmin, 293Kmin and 303Kmin, bio-char yield decreased from 63.15wt% to 42.13wt%, 59.87wt% to 38.33wt% and 51.91wt% to 32.12wt% respectively as pyrolysis temperature increased from 350℃ to 600℃. Mohan [8] used a gradual heating speed of 120 ℃/hour to produce high-yield biochar. This implies that pyrolysis with gradual heating speed can produce a high yield of biochar with higher agronomic values [19], [20]. Similarly, an increase in the temperature has an inhibitive effect on biochar yield, this is because high temperature facilitates the thermal cracking of biomass [21]. Figure 1 showed an increase in bio-oil yield from 4.15wt% to 29.65wt% at 350°C and 500°C respectively, and decreased to 27.13wt% with pyrolysis temperature of 600°C at a heating rate of 10°C/min. This decrease may be due to ash formation and as resulting from high temperature after a maximum temperature of 500°C was attained. At 20°C/min, bio-oil yield increased from 7.68wt% to 22.26wt% as the temperature rose from 350°C to 600°C and at 30°C/min, bio-oil yield decreased from 5.84wt% to 5.82wt% between 350°C and 400°C before increasing to 18.70wt% as the temperature moved from 400°C to 600°C [9].

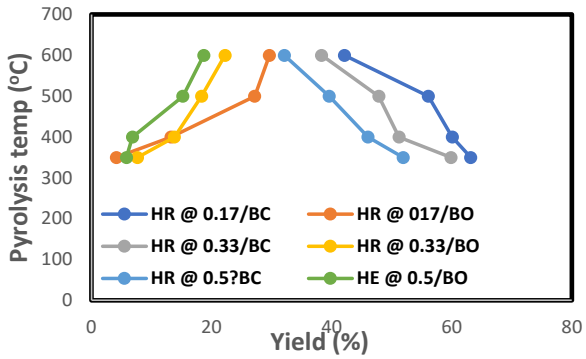

Figure 1: Effect of temperature and heating rate (HR) on the yield of biochar and bio-oil

3.3 Biochar Analysis

The composition of PPB from proximate analysis of the different biochar obtained after pyrolysis (slow) at varying temperatures and ramp values are shown in Figure 2.

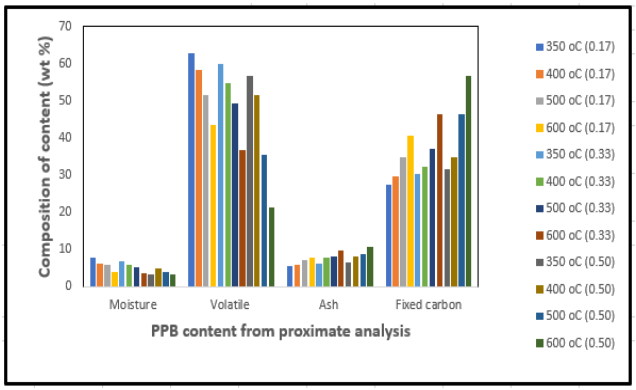

Figure 2: Biochar content from proximate analysis at different temperatures and ramp rates

The moisture content of PPB decreased with temperatures and ramp rates. The highest and lowest values were7.00 and 3.25% at 350 ℃ (0.17 ℃/sec) and 600 ℃ (0.50 ℃/sec) respectively. An efficient thermal degradation with a highly volatile matter requires an additional secondary air supply. Thus, biochar must go through additional thermal processing before being used for energy conversion. As shown in Figure 2, the volatile matter concentration was reduced from 73.10wt% to 43.66wt%, 38.18wt%, and 21.32wt% ramped at 0.17, 0.33 and 0.50 ℃/sec. respectively. At 350°C, the volatile matter concentr-ation was reduced from 73.10wt% to 62.82wt%, 59.93wt% and 56.62wt% at 283k/min, 293K/min and 303K/min respectively. The ash represents the stable and incombustible fraction of biochar. In addition, at 350 °C, the ash concentration increased from 2.56wt% to 5.6wt%, 6.10wt%, and 6.70wt% at 0.17, 0.33 and 0.50 ℃/sec respectively. Ash content also increased to 7.70wt%, 9.70wt%, and 10.80wt% for each of the heating rates. According to Venderbosch et al. [9], an increase in ash content at higher temperatures may be related to the constant concentration of mineral compositions. Low ash contents are likely preferred because high ash content in fuel often affects boiler efficiency since it causes more ash to accumulate on heat transmission surfaces [10]. Additionally, the increased ash level could make combustion's fouling and slagging issues worse. Additionally, upon pyrolysis at 350°C, the fixed carbon increased from 12.50wt% to 27.54wt%, 30.41wt%, and 31.61wt% for heating rates of 10°C/min, 20°C/min, and 30°C/min. At a maximum temperature of 600°C, higher fixed carbon contents of 40.50wt%, 46.23wt%, and 56.62wt% were obtained. By removing more volatile chemicals at higher pyrolysis temperatures, more carbon is produced during secondary carbonization reactions, which

raises the fixed carbon content [9], [22]. Overall, fixed carbon is a significant metric that determines fuel and combustion characteristics [12].

3.4 Thermal Analysis

The thermal behaviour of biochar synthesized at 500 °C was examined by the evaluation of the mass loss and derivative thermogravimetric (DTG) characteristics. The flow of N_2 gas was 10mL/min and the temperatures were ramped rates of 283, 293 and 303 K/min as shown in Figure 3 (a and b). The thermogravimetric (TGA) plots each constitute three segments. The first lies between 0 and 190°C and it is associated with the elimination of water and other light volatiles. The maximum mass loss of moisture at this region for the three heating rates is an average of 4%, which indicates the suitability of the pumpkin pod as a suitable feedstock for biochar [23]. Between 198°C and 590°C is the second phase of the pyrolysis. There was a rapid increase in the rate of decomposition of the biochar coupled with the increase in degradation rate and temperature. The maximum rate of degradation of biochar increases faster than the other regions following the publication of [19].

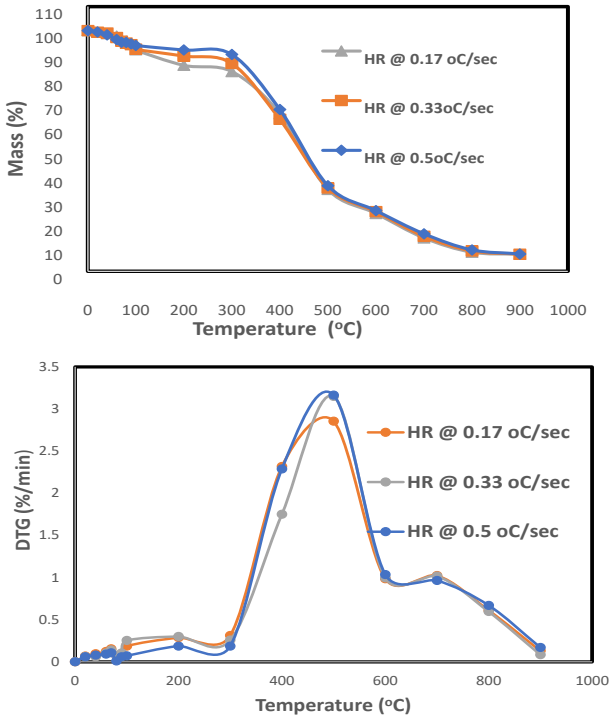

Figure 3: **(a)** TGA curve at 500°C **(b)** DTG curve at 500°C

The mass losses were 65.50%, 63.17% and 67.23% at 0.17, 0.33 and 0.50 °C/sec respectively, which are due to the heat degradation of cellulose and hemicellulose [11]. Furthermore, at 590°C to 900°C speedy degradation occurs due to the decomposition of the remains of cellulose and lignin [3]. Similarly, there is a marked decrease in the rate of degradation from 850°C to 900°C with ash contents of 8.88%, 8.21% and 7.11% at 0.17, 0.13 and 0.5 °C/sec respectively.

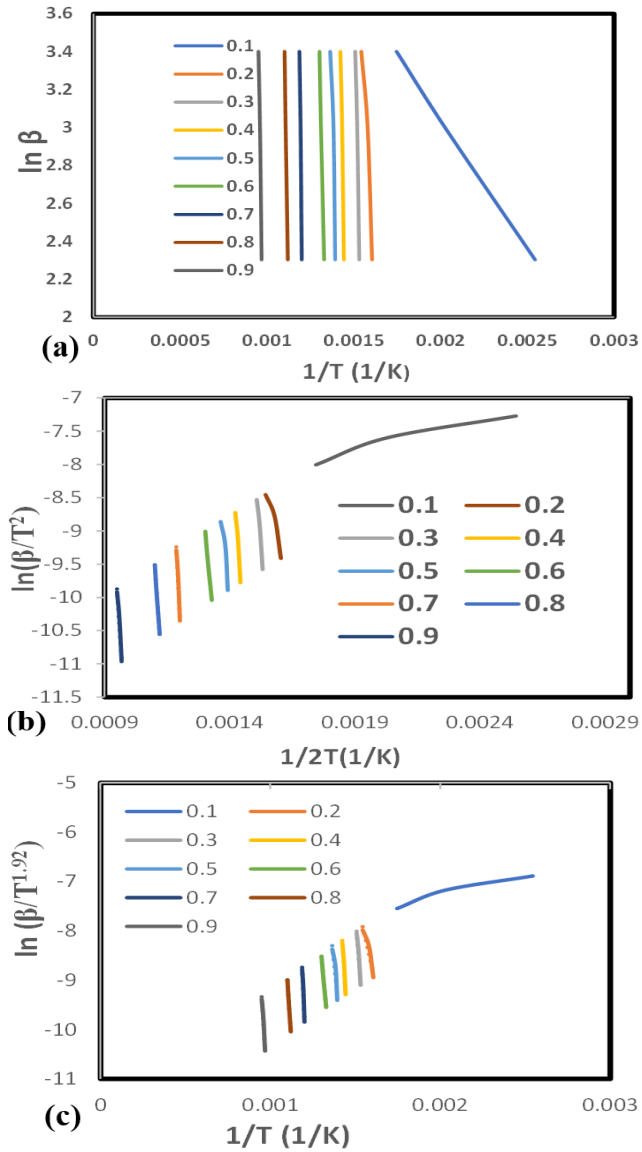

Figure 4: Plots of the **(a)** FWO **(b)** KAS and **(c)** Starink models of the biochar pyrolyzed at 500 °C

3.5 Kinetic Analysis

The change in activation energy (with conversion is represented in Figure 4 (a, b and c). The gradients of the straight lines at different conversion were used to calculate the activation energies as discussed in Equations (9), (10) and (11). Chemical reactions will not occur except when the reactants are energized to the extent that atoms become excited and either leave or cleave to one another. The energy required to achieve this is the activation energy. Table 2 shows the kinetic parameter evaluated by three models, FWO, KAS and the Starink models. The correlation

coefficients, R^2 for FWO is $0.9798 < R^2 < 0.9979$, KAS is $0.9521 < R^2 < 0.9988$ and Starink is $0.9438 < R^2 < 0.9977$. The values of R^2 of the FWO and KAS models are both higher than 0.940, this confirms an almost perfect linear fit of reduced error in the calculated. The activation energy obtained from FWO, KAS and Starink models ranged between 16.66kJ/mol to 277.35kJ/mol, 16.01kJ/mol to 267.43kJ/mol, and 16.98kJ/mol to 269.23kJ/mol respectively. The high variation between the E_A at low (16.01 to 45.42 kJ/mol) and high (127.50 to 277.89 kJ/mol)compositions may be due to a high the process being dominated by the decomposition of easily degradable constituents like hemicellulose and some parts cellulose The averages of the E_A are 157.68 kJ/mol, 157.23 kJ/mol, and 157.89 kJ/mol respectively. The average values of the E_A obtained are comparable to the values obtained by Singh et al [32] in the pyrolysis of corn cob with average E_A values of 159 (FWO), 156 (KAS) and 148 kJ/mol (Starink). The activation energies E_A of the KAS and Starink models were somewhat higher than those of the FWO model.

Table 2: Activation Energies of PPB-500 at different composition from FWO, KAS and Starink models

	FWO				KAS			Starink		
x	B (°C/sec)	E_A (kJ/mol)	R^2	A (K^{-1})	E_A (kJ/mol)	R^2	A (K^{-1})	E_A (kJ/mol)	R^2	A (K^{-1})
0.1	0.17	16.66	0.9808	5.31×10^5	16.01	0.9976	5.31×10^{05}	16.87	0.9976	5.33×10^5
	0.33			9.62×10^6			9.62×10^{06}			9.62×10^6
	0.50			1.30×10^{06}			1.30×10^{06}			1.30×10^{06}
0.2	0.17	45.03	0.9407	1.49×10^{10}	44.79	0.9971	1.49×10^{10}	45.42	0.9435	
	0.33			2.06×10^{10}			2.06×10^{10}			
	0.50			4.48×10^{10}			4.48×10^{10}			
0.3	0.17	128.70	0.9798	7.90×10^{15}	128.27	0.9521	7.90×10^{15}	128.84	0.9778	7.90×10^{15}
	0.33			1.58×10^{17}			1.58×10^{17}			1.58×10^{17}
	0.50			2.37×10^{17}			2.37×10^{17}			2.37×10^{17}
0.4	0.17	147.42	0.9796	3.57×10^{19}	153.28	0.9805	3.57×10^{19}	136.26	0.9778	3.57×10^{19}
	0.33			7.141×10^{19}			7.141×10^{19}			7.14×10^{19}
	0.50			1.07×10^{20}			1.07×10^{20}			1.07×10^{20}
0.5	0.17	156.41	0.9794	1.70×10^{20}	158.84	0.9788	1.70×10^{20}	156.89	0.9881	1.70×10^{20}
	0.33			3.56×10^{20}			3.56×10^{20}			3.56×10^{20}
	0.50			5.34×10^{20}			5.34×10^{20}			5.34×10^{20}
0.6	0.17	238.58	0.9977	2.41×10^{21}	239.21	0.8816	2.41×10^{21}	170.08	0.9975	2.41×10^{21}
	0.33			4.83×10^{21}			4.83×10^{21}			4.83×10^{21}
	0.50			7.24×10^{21}			7.24×10^{21}			7.24×10^{21}
0.7	0.17	225.50	0.9791	5.02×10^{22}	233.63	0.9988	5.02×10^{22}	226.42	0.9778	5.02×10^{22}
	0.33			9.62×10^{23}			9.62×10^{23}			9.62×10^{23}
	0.50			1.44×10^{23}			1.44×10^{23}			1.44×10^{23}
0.8	0.17	257.35	0.9979	4.59×10^{25}	261.43	0.9762	4.59×10^{25}	277.85	0.9977	4.59×10^{25}
	0.33			9.18×10^{25}			9.18×10^{25}			9.18×10^{25}
	0.50			1.37×10^{26}			1.37×10^{26}			1.37×10^{26}
	0.17	258.4	0.9798	7.95×10^{27}	254.62	0.9962	7.95×10^{27}	257.95	0.9778	7.95×10^{27}
	0.33			1.59×10^{28}			1.59×10^{28}			1.59×10^{28}
0.9	0.50			2.38×10^{28}			2.38×10^{28}			2.38×10^{28}
Average		157.23			157.68			157.38		

Figure 5 represents the E_a - X plots for all the models studied. The (E_A) showed a continual increase with conversion, except at some point where there was a decline. The slight increase of 0.1 to 0.2 may be due to the removal of moisture. More so, from 0.3 – 0.6, there is a rapid increase which may be due to the presence of volatiles, and the breakdown of the hemicellulose and cellulose [3]. The increase in E_A at the latter end may be due to the high energy needed for the degradation of the lignin, which has higher molecular masses than the cellulose [3], [24].

3.6 Estimation of Thermodynamics Parameters

The parameters of the thermodynamics behaviour of biochar at 500 °C derived from FWO, KAS and Starink models at different heating rates are shown in Table 3.

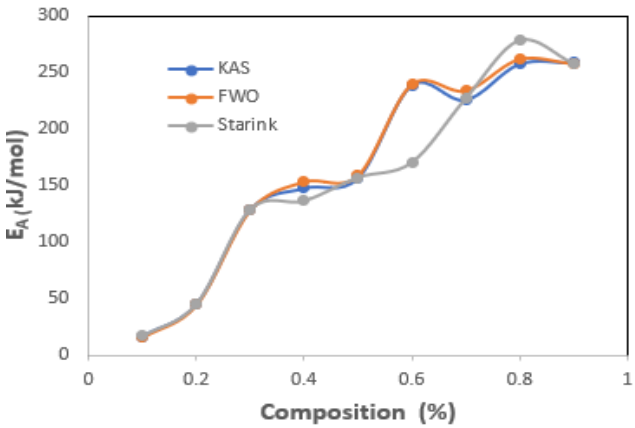

Figure 5: Variation of E_A values with conversion

Essentially, the enthalpy (ΔH), the Gibbs free energy and the entropy are key properties of thermochemical reactions. This means that positive values of ΔH ind-

icate that the reaction is endothermic. In this case, low E_A of 16.23 and 16.01 at 100 °C is an indication a of low energy barrier of the reaction at the beginning [21]. The ΔH computed from FWO, KAS and Starink models were within the limit of 20.12 to 253.49 kJ/mol, 20.2 to 252.02 kJ/mol, and 20.47 to 230.98kJ/kmol, while the mean ΔH are 152.30, 157.44 and 155.14 kJ/mol, respectively. Furthermore, the difference between ΔH and E_A with the FWO, KAS and Starink models shows that it is between 4kJ/mol and 10kJ/mol at the same extent of reaction. This implies an exceptional high reactive and spontaneous process which induces activation complexes with minimal energy [12]. The thermochemical changes which occur in the pyrolysis of biomass and the production of active complexes are functions of ΔG. The ΔG computed using FWO, KAS and Starink models (Table 3) ranged from 19.26 to 140.17kJ/mol, 18.32 to 143kJ/mol and 19.04 to 145.73kJ/mol. The mean ΔG are 112.89kJ/mol, 122.77k and 116.73kJ/mol respectively. The stability of the pyrolytic energy production of PP was confirmed by the low value of ΔG (5kJ/kmol) between two successive temperatures. This difference was not observed at 100 and 120°C in all of the models [25]. The extent of disorder and randomness of the reaction is defined by the entropy (ΔS). Low values of ΔS are confirmations of physical reaction, while higher values of ΔS implies the that chemical reaction is dominant and complexes are formed FWO, KAS and Starink models, ranged from 0.004kJ/mol/K to 0.20kJ/mol/K, and 0.0045kJ/mol/K to 0.22kJ/mol/K and 0.0049kJ/mol/K to 0.20kJ/mol/K respectively.

Values of of entropy greater than zero are indicative of a greater degree of disorder in the as the products are being formed than at the initial reaction stage. At 70% conversion, there was a large increase in enthalpy of approximately 0.2kJ/mol for all of the models, indicating that the system has greater disorder at the end of the pyrolysis reaction and the pyrolysis reaction has difficulty reaching thermodynamic equilibrium [4], [15].

Positive values of entropy indicate that the degree of disorder during the pyrolysis reaction (i.e., product) was larger than that of the initial reactants. Significantly, when the conversion rate is above 0.7, the entropy shows a large increase, indicating that the system has greater disorder at the end of the pyrolysis reaction and the pyrolysis reaction has difficulty reaching thermodynamic equilibrium [4], [15].

Table 3: Thermodynamics Parameters of PPBC at 500 °C

Composition	FWO			KAS			Starink		
	ΔH (kJ/mol)	ΔG (kJ/mol)	ΔS (kJ/mol)	ΔH (kJ/mol)	ΔG (kJ/mol)	ΔS (kJ/mol)	ΔH (kJ/mol)	ΔG (kJ/mol)	ΔS (kJ/mol)
0.1	20.12	18.32	0.0046	20.44	19.26	0.0045	20.47	19.03	0.0049
0.2	48.96	46.21	0.0041	45.18	47.84	0.004	47.32	46.77	0.0046
0.3	134.56	143.64	0.0098	132.49	146.12	0.0093	134.40	144.69	0.01
0.4	154.79	143.29	0.01	155.81	146.00	0.01	154.19	145.73	0.01
0.4	164.51	141.47	0.06	164.21	146.85	0.06	165.01	143.99	0.061
0.6	230.64	139.21	0.122	232.11	139.88	0.12	230.98	139.68	0.122
0.7	229.91	134.55	0.23	230.02	133.50	0.22	230.23	133.75	0.20
0.8	253.49	137.82	0.191	252.92	133.82	0.19	252.73	136.50	0.19
0.9	160.66	141.22	0.0611	161.20	140.17	0.06	160.94	140.42	0.0612
Average	152.30	112.89	0.077	157.44	122.77	0.076	155.14	116.73	0.074

4.0 CONCLUSION

The consequences of temperatures and rates of heating on the pyrolysis process towards the derivation of bio-oil and bio-char from pumpkin pods were evaluated. Pyrolysis temperatures of 350 °C, 400 °C, 500 °C and 600 and heating rates of 0.17, 0.33 and 0.50 °C/sec yielded biochar and bio-oil. Compared to the biomass, the bio-char had more fixed carbon and less volatile matter. The yield of the biochar and bio-oil was found to decrease with rise in temperature and heating rate. The kinetics of pyrolysis examined using Flynn–Wall– Ozawa (FWO), Kissinger–Akahira–Sunose (KAS) and Starink models showed high significance at 95% confidence level (i.e., R^2 for FWO is $0.9798 < R^2 < 0.9979$, KAS is $0.9521 < R^2 < 0.9988$ and Starink is $0.9438 < R^2 < 0.9977$). Overall, R^2 values obtained indicate a good fit for the three models while the trend in the activation energy(s) for FWO and KAS show a continual increase with the conversion of pumpkin pod to bio-char. The thermodynamic analysis showed that the process involves an endothermic reaction, with stable energy output, reactive but with little or no disorderliness. In other words, the pumpkin pod is a suitable biomass for energy derivation. Its availability as food waste and zero competition for food makes it a dependable sustainable energy feedstock, with no deforestation when compared to other biomasses and adds to other existing energy resources (mix) for bio-char and/or bio-oil production.

REFERENCES

[1] Demirbas, A. "The influence of temperature on the yields of compounds existing in bio-oils obtained from biomass samples via pyrolysis," *Fuel Processing Technology*, vol. 88, no. 6, pp. 591–597, Jun. 2007, doi: 10.1016/j.fuproc.2007.01.010.

[2] Ajieh, M. U., Isagba, E. S., Ihoeghian, N., Edosa, V. I. O., Amenaghawon, A., Oshoma, C. E., Erhunmwunse, N., Obuekwe, I. S., Tongo, I., Emokaro, C., and Ezemonye, L. I. N. "Assessment of sociocultural acceptability of biogas from faecal waste as an alternative energy source in selected areas of Benin City, Edo State, Nigeria", *Environment, Development and Sustainability*, 2021. https://doi.org/10.1007/s10668-020-01205-y

[3] Dhyani, V., and Bhaskar, T. "A comprehensive review on the pyrolysis of lignocellulosic biomass," *Renew Energy*, vol. 129, pp. 695–716, Dec. 2018, doi: 10.1016/j.renene.2017.04.035.

[4] García, R., Pizarro, C., Lavín, A. G., and Bueno, J. L. "Biomass proximate analysis using thermogravimetry," *Bioresour Technol*, vol. 139, pp. 1–4, 2013, doi: 10.1016/j.biortech.2013.03.197.

[5] Ajieh, M. U., Owamah, H. I., Edomwonyi-Otu, L. C., Ajieh, G. I., Aduba, P., Owebor, K., and Ikpeseni, S. C. "Characteristics of fuelwood perturbation and effects on carbon monoxide and particulate pollutants emission from cookstoves in Nigeria," *Energy for Sustainable Development*, vol. 72, pp. 151–161, Feb. 2023, doi: 10.1016/j.esd.2022.12.008.

[6] Ren, G., Xu, X., Qu, J., Zhu, L., and Wang, T. "Evaluation of microbial population dynamics in the co-composting of cow manure and rice straw using high throughput sequencing analysis," *World J Microbiol Biotechnol*, vol. 32, no. 6, Jun. 2016, doi: 10.1007/s11274-016-2059-7.

[7] Feng, Q., and Lin, Y. "Integrated processes of anaerobic digestion and pyrolysis for higher bioenergy recovery from lignocellulosic biomass: A brief review," *Renewable and Sustainable Energy Reviews*, vol. 77. Elsevier Ltd, pp. 1272–1287, 2017. doi: 10.1016/j.rser.2017.03.022.

[8] Mohan, D., Pittman, C. U., and Steele, P. H. "Pyrolysis of wood/biomass for bio-oil: A critical review," *Energy and Fuels*, vol. 20, no. 3. pp. 848–889, May 2006. doi: 10.1021/ef0502397.

[9] Venderbosch, R. H., Ardiyanti, A. R., Wildschut, J., Oasmaa, A., and Heeres, H. J. "Stabilization of biomass-derived pyrolysis oils," *Journal of Chemical Technology and Biotechnology*, vol. 85, no. 5, pp. 674–686, 2010, doi: 10.1002/jctb.2354.

[10] Kocbach, A., Li, Y., Yttri, K. E., Cassee, F. R., Schwarze, P. E., and Namork, E. "Physicochemical characterisation of combustion particles from vehicle exhaust and residential wood smoke," *Part Fibre Toxicol*, vol. 3, Jan. 2006, doi: 10.1186/1743-8977-3-1.

[11] Singh, H., and Jain, A. K. "Ignition, combustion, toxicity, and fire retardancy of polyurethane foams: A comprehensive review," *J Appl Polym Sci*, vol. 111, no. 2, pp. 1115–1143, Jan. 2009, doi: 10.1002/app.29131.

[12] Arenas, C. N., Navarro, M. V., and Martínez, J. D. "Pyrolysis kinetics of biomass wastes using isoconversional methods and the distributed activation energy model," *Bioresour Technol*, vol. 288, Sep. 2019, doi: 10.1016/j.biortech.2019.121485.

[13] Ungureanu, N., Vladut, V., Voicu, G., Dinca, M. N. and Zabava, B. S. "Influence of biomass moisture content on pellet properties - Review," in *Engineering for Rural Development*, Latvia University of Agriculture, 2018, pp. 1876–1883. doi: 10.22616/ERDev2018.17.N449.

[14] Lozano-Martín, D., Vega-Maza, D., Moreau, A., Martín, M. C., Tuma, D., and Segovia, J. J. "Speed of sound data, derived perfect-gas heat capacities, and acoustic virial coefficients of a calibration standard natural gas mixture and a low-calorific H2-enriched mixture," *Journal of Chemical Thermodynamics*, vol. 158, 2021, doi: 10.1016/j.jct.2021.106434.

[15] García-Maraver, A., Popov, V., and Zamorano, M. "A review of European standards for pellet quality," *Renew Energy*, vol. 36, no. 12, pp. 3537–3540, Dec. 2011, doi: 10.1016/j.renene.2011.05.013.

[16] Garg, R., Anand, N., and Kumar, D. "Pyrolysis of babool seeds (Acacia nilotica) in a fixed bed reactor and bio-oil characterization," *Renew Energy*, vol. 96, pp. 167–171, Oct. 2016, doi: 10.1016/j.renene.2016.04.059.

[17] Ihoeghian, N. A., Amenaghawon, A. N., Ogofure, A., Oshoma, C. E., Ajieh, M. U., Erhunmwunse, N. O., Obuekwe, I. S., Edosa, V. I. O., Tongo, I., Emokaro, C., Ezemonye, L. I. N., Semple, K. T., and Martin, A. D. "Biochar-facilitated batch co-digestion of food waste and cattle rumen content: An assessment of process stability, kinetic studies, and pathogen fate," *Green Technologies and*

Sustainability, vol. 1, no. 3, p. 100035, Sep. 2023, doi: 10.1016/j.gre ts.2023.100035.

[18] Isagba, E. S., Ajieh, M. U., Oshoma, C. E., Amenaghawon, A., Ogofure, A., Obatusin, V., Obuekwe, I. S., Tongo, I., Ihoeghian, N., Edosa, V. I. O., Erhunmwunse, N., Lag-Brotons, A. J., Emokaro, C., Ezemonye, L. I. N., and Semple, K. T. "Assessment of Anaerobic Digestate Amended with Wood Ash and Green Vegetable Matter and Impacts on Microbial Growth," *Waste Biomass Valorization*, 2023, doi: 10.1007/s12649-023-02055-1.

[19] Liu, Z., and Han, G. "Production of solid fuel biochar from waste biomass by low temperature pyrolysis," *Fuel*, vol. 158, pp. 159–165, May 2015, doi: 10.1016/j.fuel.2015.05.032.

[20] Azeem, M., Hale, L., Montgomery, J., Crowley, D., and McGiffen, M. E. "Biochar and compost effects on soil microbial communities and nitrogen induced respiration in turfgrass soils," *PLoS One*, vol. 15, no. 11 November, Nov. 2020, doi: 10.1371/journal.pone.0242209.

[21] Dhaundiyal, A., and Gangwar, J. "Kinetics of the thermal decomposition of pine needles," *Acta Universitatis Sapientiae, Agriculture and Environment*, vol. 7, no. 1, pp. 5–22, Dec. 2015, doi: 10.1515/ausae-2015-0001.

[22] Mythili, R., Venkatachalam, P., Subramanian, P., and Uma, D. "Characterization of bioresidues for biooil production through pyrolysis," *Bioresour Technol*, vol. 138, pp. 71–78, 2013, doi: 10.1016/j.biortech.2013.03.161.

[23] Kirch, T., Medwell, P. R., Birzer, C. H., and van Eyk, P. J. "Feedstock Dependence of Emissions from a Reverse-Downdraft Gasifier Cookstove," *Energy for Sustainable Development*, vol. 56, pp. 42–50, Jun. 2020, doi: 10.1016/j.esd.2020.02.008.

[24] Fahmi, R., Bridgwater, A. V., Donnison, I., Yates, N., and Jones, J. M. "The effect of lignin and inorganic species in biomass on pyrolysis oil yields, quality and stability," *Fuel*, vol. 87, no. 7, pp. 1230–1240, Jun. 2008, doi: 10.1016/j.fuel.2007.07.026.

[25] Das, S., Ghosh, S., Kuila, T., Murmu, N. C., and Kundu, A. "Biomass-Derived Advanced Carbon-Based Electrocatalysts for Oxygen Reduction Reaction," *Biomass*, vol. 2, no. 3, pp. 155–177, Aug. 2022, doi: 10.3390/biomass2030010.

[26] Bareschino, P., Marrasso, E., and Roselli, C. "Tobacco stalks as a sustainable energy source in civil sector: Assessment of techno-economic and environmental potential", *Renewable Energy*, *175*, 373–390; 2021. https://doi.org/10.1016/j.r enene.2021.04.101

[27] Ajieh, M. U., Ogbomida, E. T., Uhunamure, N. D., Agbale, R. N., Ajieh, G. I., Ekperi, R., Owamah, H. I., and Okafor, I. F. "Analytical assessment of knowledge, attitude and practices (KAP) of waste management practices to optimize energy and food nexus: A case study of Oleh, Isoko South LGA, Delta State, Nigeria", *African Journal of Environmental Science and Technology*, *18*(8), 170–186; 2024. https://doi.org/10.5897/ajest2024.3275

[28] Arenas, C. N., Navarro, M. V., and Martínez, J. D. "Pyrolysis kinetics of biomass wastes using isoconversional methods and the distributed activation energy model", *Bioresource Technology*, *288*, pp. 1-34; 2019. https://doi.org/10.1016/j.biortech.2019.121485

[29] Bianchi, O., Oliveira, R. V. B., Fiorio, R., Martins, J. D. N., Zattera, A. J., and Canto, L. B. "Assessment of Avrami, Ozawa and Avrami-Ozawa equations for determination of EVA crosslinking kinetics from DSC measurements", *Polymer Testing*, *27*(6), 722–729; 2008. https://doi.org/10.1016/j.polymertesting.2008.05.003

[30] Lim, A. C. R., Chin, B. L. F., Jawad, Z. A., and Hii, K. L. "Kinetic Analysis of Rice Husk Pyrolysis Using Kissinger-Akahira-Sunose (KAS) Method", *Procedia Engineering*, *148*, 1247–1251; 2016. https://doi.org/10.1016/j.proeng.2016.06.486

[31] Yan, J., Yang, Q., Zhang, L., Lei, Z., Li, Z., Wang, Z., Ren, S., Kang, S., and Shui, H. "Investigation of kinetic and thermodynamic parameters of coal pyrolysis with model-free fitting methods", *Carbon Resources Conversion*, *3*, 173–181; 2020. https://doi.org/10.1016/j.crcon.2020.11.002

[32] Singh, S., Patil, T., Tekade, S. P., Gawande, M. B., and Sawarkar, A. N. "Studies on individual pyrolysis and co-pyrolysis of corn cob and polyethylene: Thermal degradation behavior, possible synergism, kinetics, and thermodynamic analysis", *Science of the Total Environment*, *783*, 2021. https://doi.org/10.1016/j.scitotenv.2021.147004